

Experimental Observations of Group Synchrony in a System of Chaotic Optoelectronic Oscillators

Caitlin R. S. Williams,^{1,2} Thomas E. Murphy,^{1,3} Rajarshi Roy,^{1,2,4}
 Francesco Sorrentino,⁵ Thomas Dahms,⁶ and Eckehard Schöll⁶

¹*Institute for Research in Electronics and Applied Physics, University of Maryland, College Park, Maryland 20742, USA*

²*Department of Physics, University of Maryland, College Park, Maryland 20742, USA*

³*Department of Electrical and Computer Engineering, University of Maryland, College Park, Maryland 20742, USA*

⁴*Institute for Physical Science and Technology, University of Maryland, College Park, Maryland 20742, USA*

⁵*Department of Mechanical Engineering, University of New Mexico, Albuquerque, New Mexico 87131, USA*

⁶*Institut für Theoretische Physik, Technische Universität Berlin, 10623 Berlin, Germany*

(Received 11 October 2012; published 6 February 2013; corrected 28 March 2013)

We experimentally demonstrate group synchrony in a network of four nonlinear optoelectronic oscillators with time-delayed coupling. We divide the nodes into two groups of two each, by giving each group different parameters and by enabling only intergroup coupling. When coupled in this fashion, the two groups display different dynamics, with no isochronal synchrony between them, but the nodes in a single group are isochronally synchronized, even though there is no intragroup coupling. We compare experimental behavior with theoretical and numerical results.

DOI: [10.1103/PhysRevLett.110.064104](https://doi.org/10.1103/PhysRevLett.110.064104)

PACS numbers: 05.45.Xt, 89.75.-k

The past years have seen a vast increase in the interest in coupled dynamical systems, ranging from a few coupled elements to complex networks [1,2]. Besides the focus on network structure and topology, the research area of synchronization in networks has grown rapidly [3,4]. The groundbreaking work on the *master stability function* (MSF) by Pecora and Carroll has bridged the gap between topology and dynamics by allowing predictions about synchronization based solely on the nodes' dynamics and the eigenvalue spectrum of the coupling matrix [5].

While the MSF theory was originally developed for identical, isochronous synchronization, more complex patterns of synchronization are observed in applications in, e.g., neural systems, genetic regulation, or optical systems [6–15]. These patterns include, for example, sublattice synchronization in coupled loops of identical oscillators with heterogeneous delays [16], pairwise synchronization of pairwise identical nodes coupled through a common channel [17], and more general group synchronization [18]. *In group synchronization, the local dynamics in synchronized clusters can be different from the dynamics in the other cluster(s)*, which extends the possibility of synchronization behavior to networks formed of heterogeneous dynamical systems, as they appear in a variety of applications. Moreover, these synchronous patterns can be observed even when there is no intragroup coupling. Sorrentino and Ott have generalized the MSF approach to group synchronization [18], and recent work by Dahms, Lehnert, and Schöll considers time-delayed coupling of an arbitrary number of groups [19].

In this Letter, we demonstrate the successful realization of group synchronization of chaotic dynamics in an array of four optoelectronic oscillators. Optoelectronic oscillators

with time-delayed feedback have been found to show a multitude of different dynamical behaviors ranging from steady-state to chaotic dynamics depending on parameters [20–25]. In this work we experimentally demonstrate group synchrony, where the two groups display different fluctuation amplitudes. Remarkably, the synchronized oscillators in one group are not directly coupled to each other; they are coupled only to those of the other group.

The experimental setup consists of four optoelectronic feedback loops, which act as the four nodes of the network. We consider several coupling schemes. In the first one, the nodes are coupled together in the configuration shown in Fig. 1(a) in order to form two groups. There are no direct coupling links between two nodes in the same group. However, a node is coupled bidirectionally to both of the nodes in the other group. In this experiment, the coupling strength ε and coupling delay τ are the same for all coupling links. However, the parameters of the nodes differ depending on which group the nodes are in. Both of the nodes in group A are identical, and both of the nodes in group B are identical, but the nodes in group A are not identical to the nodes in group B. In Fig. 1(a), the coupling links are shown in black (arrows in each direction to indicate bidirectional coupling), and the self-feedback of the nodes is indicated by the gray (colored) lines and arrows.

A schematic of a single node is shown in Fig. 1(b), where red lines indicate optical fibers, and black or green lines indicate electronic paths. In each node, light from a diode laser passes through a Mach-Zehnder modulator (MZM), whose output light intensity is $\cos^2(x + \phi_0)$ for an input voltage signal x . There is a controllable bias phase of the MZM, which we set to be $\phi_0 = \frac{\pi}{4}$. The optical signal is split into three equal signals: One is the feedback

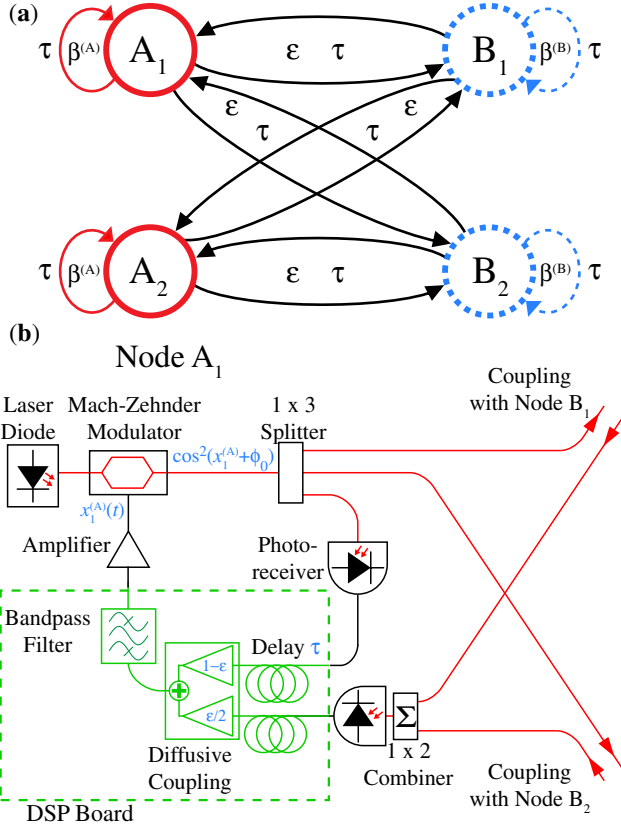


FIG. 1 (color online). (a) Schematic of four nodes separated into two groups, A (red, solid line) and B (blue, dashed line). (b) Experimental setup of a single node, showing coupling to the other nodes according to the configuration in (a).

signal, and the other two are the coupling to the two nodes in the opposite group. A photoreceiver converts the feedback optical signal to an electrical signal, which is one of the two inputs to the DSP (digital signal processing) board. The incoming optical signals from the two nodes of the other group are combined optically before a second photoreceiver converts the composite coupled signal to an electronic signal, which is the second input of the DSP board. The DSP board implements the feedback and coupling time delays, which are the same for this experiment ($\tau = 1.4$ ms), and a diffusive coupling scheme. The feedback signal is scaled by a factor of $1 - \epsilon$, while each incoming signal to a node is scaled by a factor of ϵ/n_{in} , for the global coupling strength ϵ and the number of links incoming to a node, n_{in} . For the configuration shown in Fig. 1(a), $n_{in} = 2$ for all nodes, but, in general, n_{in} can be different for each node. The feedback and coupled signals are summed on the DSP board.

The DSP board also implements a digital filter, which is a two-pole bandpass filter with cutoff frequencies at 100 Hz and 2.5 kHz and a sampling rate of 24 kSamples/s and also scales the combined signal by a scale factor, which controls the feedback strength, which we denote as β . The output of the DSP board is amplified with a

voltage amplifier, whose output drives the MZM. Although β is a combination of gains of the photoreceiver, amplifier, and other components, the DSP board is the only place where the gain is changed.

For this experiment, all parameters except for β are identical in all four nodes. We keep β identical among the members of each group but allow a different β for each group, denoted by $\beta^{(A)}$ and $\beta^{(B)}$. Previous studies have revealed the wide variety of behaviors that are possible for this type of system, depending on the value of β [22]. For this study, we have used a range of β from 0 to 10, with the experiments focusing on cases of $\beta > 3$, for which the system displays chaos (with some periodic windows) when the nodes are not coupled.

For each run of the experiment, the nodes are started from random initial conditions. This system has a time delay, so the initial condition will be a function of time. Thus, we record the random electrical activity at the input to the DSP in the absence of coupling and feedback for 1 s to provide the initial states for the nodes. After recording an initial condition, we enable feedback for 4 s, which is long enough for transients to disappear. At the end of this period, we enable coupling. Data are taken after transients have died out.

The system of coupled feedback loops can be well described by a mathematical model with a system of time delay differential equations for the voltages input to the MZMs $x_i^{(m)} \in \mathbb{R}$ and the vectors describing the states of the filters $\mathbf{u}_i^{(m)} \in \mathbb{R}^2$ [22]:

$$\dot{\mathbf{u}}_i^{(m)}(t) = \mathbf{E}\mathbf{u}_i^{(m)}(t) - \mathbf{F}\beta^{(m)}\cos^2[x_i^{(m)}(t - \tau) + \phi_0], \quad (1)$$

$$x_i^{(m)}(t) = \mathbf{G}\left[\mathbf{u}_i^{(m)}(t) + \epsilon \sum_j K_{ij}^{(m)}[\mathbf{u}_j^{(m)}(t) - \mathbf{u}_i^{(m)}(t)]\right], \quad (2)$$

where m and $m' \neq m$ denote the groups A or B, respectively, and i indicates the node within a group.

$$\mathbf{E} = \begin{pmatrix} -(\omega_H + \omega_L) & -\omega_L \\ \omega_H & 0 \end{pmatrix},$$

$$\mathbf{F} = \begin{pmatrix} \omega_L \\ 0 \end{pmatrix},$$

and

$$\mathbf{G} = \begin{pmatrix} 1 & 0 \end{pmatrix}$$

are constant matrices that describe the filter. The filter parameters are chosen as $\omega_L = 2\pi \times 2.5$ kHz and $\omega_H = 2\pi \times 0.1$ kHz. For a bipartite network with no intragroup coupling, we define the intergroup coupling matrices $\mathbf{K}^{(m)} = \{K_{ij}^{(m)}\}$:

$$\mathbf{K} = \begin{pmatrix} 0 & \mathbf{K}^{(A)} \\ \mathbf{K}^{(B)} & 0 \end{pmatrix}, \quad (3)$$

where \mathbf{K} is the overall coupling matrix for the entire network. For the configuration shown in Fig. 1(a), $i, j = 1, 2$, and

$$\mathbf{K}^{(A)} = \mathbf{K}^{(B)} = \frac{1}{2} \begin{pmatrix} 1 & 1 \\ 1 & 1 \end{pmatrix}$$

so that

$$\mathbf{K} = \begin{pmatrix} 0 & \mathbf{K}^{(A)} \\ \mathbf{K}^{(B)} & 0 \end{pmatrix} = \frac{1}{2} \begin{pmatrix} 0 & 0 & 1 & 1 \\ 0 & 0 & 1 & 1 \\ 1 & 1 & 0 & 0 \\ 1 & 1 & 0 & 0 \end{pmatrix}. \quad (4)$$

Equations (1) and (2) can describe the dynamics of the uncoupled nodes if we set the coupling strength $\varepsilon = 0$, as the second term in Eq. (2) represents the diffusive coupling scheme.

Numerical simulations use a discrete-time implementation of these differential equations, as described in Ref. [22]. The simulations of uncoupled and coupled systems are in excellent agreement with the experimental results for the variety of dynamical behaviors that can be observed.

We will now investigate the existence and stability of the group synchronous solution; i.e., we will derive analytical conditions determining whether such a solution (in which the two nodes of each group are identically and isochronously synchronized, but there is no identical synchrony between nodes of different groups) exists for given values of $\beta^{(A)}$ and $\beta^{(B)}$, and if it does, whether that solution is stable. We use the approach described in Refs. [18,19]. The condition for the existence of the group synchronous solution for a particular coupling configuration is that

$$\sum_j K_{ij}^{(m)} = c^{(m)}, \quad m = \{A, B\}, \quad (5)$$

i.e., that the row sum of the matrices $\mathbf{K}^{(m)}$ is constant. For the work reported here, we fix $c^{(A)} = c^{(B)} = 1$.

The group synchronized dynamics for group m is given by

$$\dot{\mathbf{u}}_s^{(m)}(t) = \mathbf{E} \mathbf{u}_s^{(m)}(t) - \mathbf{F} \beta^{(m)} \cos^2[x_s^{(m)}(t - \tau) + \phi_0], \quad (6)$$

$$x_s^{(m)}(t) = \mathbf{G} \{ \mathbf{u}_s^{(m)}(t) + \varepsilon [\mathbf{u}_s^{(m')}(t) - \mathbf{u}_s^{(m)}(t)] \}. \quad (7)$$

Linearizing Eqs. (1) and (2) about the synchronous solution $\mathbf{u}_s^{(m)}$ ($m = A, B$), we obtain the master stability equations:

$$\begin{aligned} \delta \dot{\mathbf{u}}^{(m)}(t) &= \mathbf{E} \delta \mathbf{u}^{(m)}(t) - \mathbf{F} \beta^{(m)} \sin[2x_s^{(m)}(t - \tau) + 2\phi_0] \\ &\quad \times \mathbf{G} [(1 - \varepsilon) \delta \mathbf{u}^{(m)}(t - \tau) + \varepsilon \gamma \mathbf{u}^{(m')}(t - \tau)]. \end{aligned} \quad (8)$$

In Eq. (8), γ is a parameter that is chosen from the eigenvalue spectrum of \mathbf{K} . The largest Lyapunov exponent as a function of this parameter γ is called the MSF. For the

configurations presented here, the nonzero eigenvalues of \mathbf{K} are 1 and -1 , and any remaining eigenvalues are zeros. Moreover, the stability results will be identical for any two-group network whose nodes are described by Eqs. (1) and (2) and whose coupling matrix is in the form of (3), satisfies (5), and has identical rows for either $\mathbf{K}^{(A)}$ or $\mathbf{K}^{(B)}$ (for a proof, see Supplemental Material [26]).

The eigenvalues $\gamma = -1$ and $\gamma = 1$ in the master stability equation (8) correspond to perturbations parallel to the synchronization manifold. The corresponding value of the MSF determines the dynamical behavior inside the synchronization manifold and is shown in Fig. 2(a) in dependence on the parameters $\beta^{(A)}$ and $\beta^{(B)}$. Negative, zero, and positive values denote fixed-point, periodic, and chaotic dynamics, respectively. Because of the inversion symmetry of the MSF for two-group synchronization [18,19], the MSF values are identical for $\gamma = -1$ and $\gamma = 1$.

Transverse stability of the synchronization manifold is determined by using the eigenvalue $\gamma = 0$ in Eq. (8). Figure 2(b) shows the largest Lyapunov exponent in the transverse direction, which is negative for almost the entire range of $\beta^{(A)}$ and $\beta^{(B)}$ that is shown, indicating that we expect the group synchronous solution to be stable for most parameters.

To observe group synchrony in this system, we select dissimilar values of $\beta^{(A)}$ and $\beta^{(B)}$, as shown by the black dots in Fig. 2. The global coupling strength is chosen as $\varepsilon = 0.8$. The experimental values for $\beta^{(A)}$ and $\beta^{(B)}$ were adjusted by using the DSP board. The values of $\beta^{(A)}$ and $\beta^{(B)}$ used in simulation were established by varying the values close to the experimental values to find nearby values which match best the dynamical behavior of the experiments for uncoupled nodes, obtained from the shape of the reconstructed attractor in phase space. Since the values determined experimentally as $\beta^{(A)} = 7.6$ and $\beta^{(B)} = 3.3$ are subject to measurement uncertainties, it is not surprising that we find slightly different values in simulation, i.e., $\beta^{(A)} = 7.66$ and $\beta^{(B)} = 3.28$. Comparison of uncoupled and coupled time traces in experiment and simulation is shown in the Supplemental Material, Fig. S1 [26].

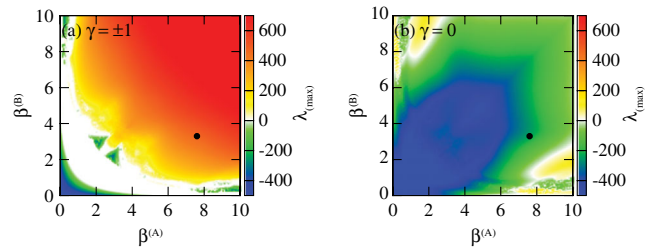


FIG. 2 (color online). Maximum Lyapunov exponent λ_{\max} as a function of $\beta^{(A)}$ and $\beta^{(B)}$: (a) in the longitudinal directions $\gamma = \pm 1$ and (b) in the transverse direction $\gamma = 0$. White areas correspond to $\lambda_{\max} = 0$. The black dot indicates values of $\beta^{(A)}$ and $\beta^{(B)}$ used in this experiment.

Figure 3 shows experimental and simulated time traces of the coupled system. The simulated traces in Fig. 3(a) show the behavior of *any* two-group system displaying stable group synchrony according to Eqs. (6) and (7), with the parameters we have used here. Figure 3(b) shows experimental results for a system coupled according to Fig. 1(a). These time traces show that there is identical, isochronal synchrony between $x_1^{(A)}$ and $x_2^{(A)}$, and between $x_1^{(B)}$ and $x_2^{(B)}$, but not identical synchrony between the groups. Thus, this is an example of group synchrony. We also performed experiments on two asymmetric four-node configurations. These configurations were created by removing links from the original structure of Fig. 1(a) while preserving the constant row sum and eigenvalues (1, -1, 0, and 0) of \mathbf{K} , keeping all other parameters the same. Their topologies and dynamics are shown in Figs. 3(c) and 3(d). Because these schemes are also described by Fig. 2, they also display group synchrony. In the experimental time traces, there are slight differences between the two traces

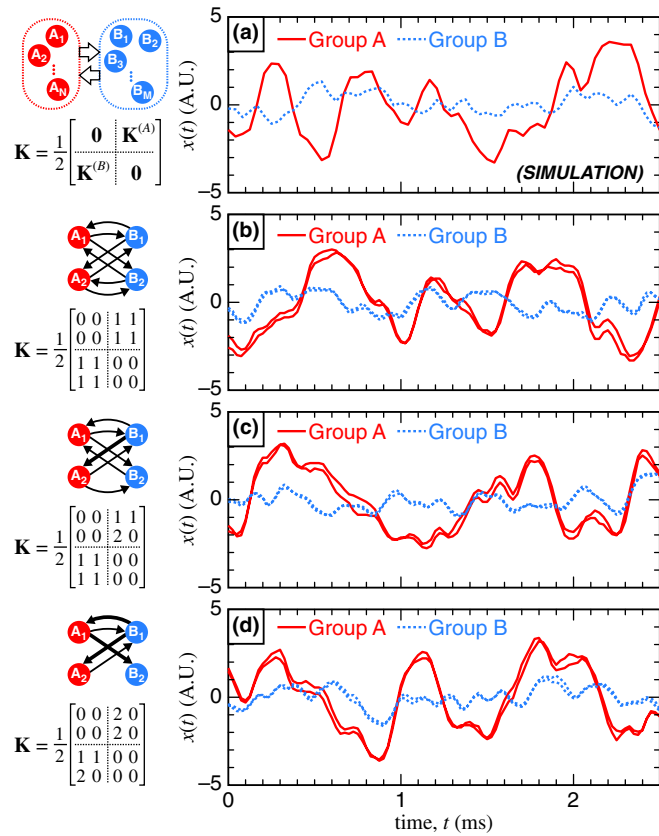


FIG. 3 (color online). (a) Simulated motion in the synchronization manifold, obtained by numerically solving Eqs. (6) and (7), showing the predicted group-synchronous state. (b)–(d) Experimentally measured time traces from three different network configurations (indicated by the coupling scheme and the coupling matrices \mathbf{K}) that achieve group synchrony. All three networks have the same eigenspectra, but the configuration in (b) is symmetric while those in (c) and (d) are not.

of one group, due to the intrinsic experimental noise and mismatch we expect in any real system. An example of a larger network that displays the same behavior is presented in the Supplemental Material, Fig. S2 [26].

To further examine the nature of the synchrony of this system, we calculate the correlation functions of the experimental time traces, as shown in Fig. 4 for the topology shown in Fig. 1(a). For two variables $y(t)$ and $z(t)$, which each have a mean of zero, we define the correlation function C as a function of time lag Δt [27]:

$$C(\Delta t) = \frac{\langle y(t)z(t + \Delta t) \rangle}{\sqrt{\langle y^2(t) \rangle \langle z^2(t) \rangle}}. \quad (9)$$

Figure 4(a) shows the autocorrelation functions for one node in each group when the nodes are uncoupled. The autocorrelation of $x_1^{(A)}$ shows only a peak at zero time lag, which indicates chaotic dynamics, while the autocorrelation of $x_1^{(B)}$ shows periodic dynamics, with correlation peaks

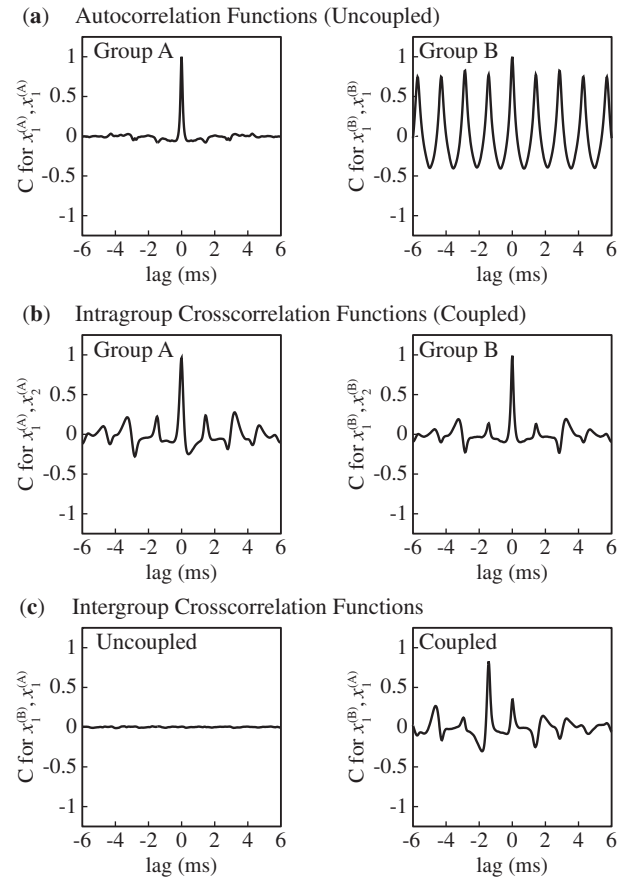


FIG. 4. Correlation functions of 3.9s of experimental data. (a) Autocorrelation functions for the dynamics of group A (left) and group B (right), with no coupling in the system. (b) Cross-correlation functions between the two nodes in group A (left) and group B (right), for coupled nodes. (c) Cross-correlation functions between one node in group A and one node in group B for the uncoupled system (left) and coupled system (right).

at intervals of the time delay $\tau = 1.4$ ms. In Fig. 4(b), we show the cross-correlation functions of $x_1^{(A)}$ with $x_2^{(A)}$ and of $x_1^{(B)}$ with $x_2^{(B)}$ for the coupled system, which confirms identical, isochronal chaotic synchronization between the two nodes in a single group. Figure 4(c) shows the cross-correlation functions between two nodes in different groups, without and with coupling. The uncoupled case has no correlation, as we expect, but the coupled case has a high correlation peak at a lag of $\Delta t = -1.4$ ms. From this, we can see that there is time-lagged phase synchrony between the two groups, with the dynamics of group B leading the dynamics of group A by the system delay τ . However, the amplitudes of fluctuations of the two groups are still different after coupling, so there is no complete synchronization, and we have an interesting situation of the simultaneous coexistence of intragroup isochronal identical synchrony and time-lagged phase synchrony between the groups.

In conclusion, we have examined a four-node system of nonlinear optoelectronic oscillators in the case where there are two groups of nodes with dissimilar parameters. Our experiments display the phenomenon of group synchronization, and we analyze the stability of the group synchronized solutions for chaotic dynamical states. It is remarkable that, although the coupling is entirely between the different groups and not within the groups, identical isochronal synchronization within each group is induced by this coupling, while the two groups are not mutually amplitude synchronized, as predicted by our stability analysis using the generalized master stability function [18,19]. Thus the nodes of group B act as a kind of dynamical relay [28] for the nodes of group A, and vice versa. These results have been experimentally demonstrated with three coupling configurations, and conditions for observing group synchrony in other networks have been discussed.

Our observations go beyond previous work on sublattice and cluster synchrony, where the experiments focused on optical phase synchronization for coupled lasers without self-feedback [9,10]. Group synchronization in larger networks is a significant challenge for future experimental investigation.

This work was supported by DOD MURI Grant No. ONR N000140710734 and by DFG in the framework of SFB 910. The authors acknowledge helpful comments from I. Kanter and L. Pecora.

-
- [1] R. Albert and A.-L. Barabási, *Rev. Mod. Phys.* **74**, 47 (2002).
 [2] S. Boccaletti, V. Latora, Y. Moreno, M. Chavez, and D.-U. Hwang, *Phys. Rep.* **424**, 175 (2006).
 [3] L. M. Pecora and T. L. Carroll, *Phys. Rev. Lett.* **64**, 821 (1990).

- [4] A. S. Pikovsky, M. G. Rosenblum, and J. Kurths, *Synchronization, A Universal Concept in Nonlinear Sciences* (Cambridge University Press, Cambridge, England, 2001).
 [5] L. M. Pecora and T. L. Carroll, *Phys. Rev. Lett.* **80**, 2109 (1998).
 [6] J. M. Buldu, M. C. Torrent, and J. Garcia-Ojalvo, *J. Lightwave Technol.* **25**, 1549 (2007).
 [7] C. M. González, C. Masoller, M. C. Torrent, and J. García-Ojalvo, *Europhys. Lett.* **79**, 64003 (2007).
 [8] J. Kestler, W. Kinzel, and I. Kanter, *Phys. Rev. E* **76**, 035202 (2007).
 [9] Y. Aviad, I. Reidler, M. Zigzag, M. Rosenbluh, and I. Kanter, *Opt. Express* **20**, 4352 (2012).
 [10] M. Nixon, M. Friedman, E. Ronen, A. A. Friesem, N. Davidson, and I. Kanter, *Phys. Rev. Lett.* **106**, 223901 (2011).
 [11] A. Amann, A. Pokrovskiy, S. Osborne, and S. O'Brien, *J. Phys. Conf. Ser.* **138**, 012001 (2008).
 [12] S. Pigolotti, S. Krishna, and M. H. Jensen, *Proc. Natl. Acad. Sci. U.S.A.* **104**, 6533 (2007).
 [13] M. H. Jensen, S. Krishna, and S. Pigolotti, *Phys. Rev. Lett.* **103**, 118101 (2009).
 [14] C.-U. Choe, T. Dahms, P. Hövel, and E. Schöll, *Phys. Rev. E* **81**, 025205 (2010).
 [15] I. Kanter, E. Kopelowitz, R. Vardi, M. Zigzag, W. Kinzel, M. Abeles, and D. Cohen, *Europhys. Lett.* **93**, 66001 (2011).
 [16] I. Kanter, M. Zigzag, A. Englert, F. Geissler, and W. Kinzel, *Europhys. Lett.* **93**, 60003 (2011).
 [17] J. Kestler, E. Kopelowitz, I. Kanter, and W. Kinzel, *Phys. Rev. E* **77**, 046209 (2008).
 [18] F. Sorrentino and E. Ott, *Phys. Rev. E* **76**, 056114 (2007).
 [19] T. Dahms, J. Lehnert, and E. Schöll, *Phys. Rev. E* **86**, 016202 (2012).
 [20] Y. C. Kouomou, P. Colet, L. Larger, and N. Gastaud, *Phys. Rev. Lett.* **95**, 203903 (2005).
 [21] M. Peil, M. Jacquot, Y. K. Chembo, L. Larger, and T. Erneux, *Phys. Rev. E* **79**, 026208 (2009).
 [22] T. E. Murphy, A. B. Cohen, B. Ravoori, K. R. B. Schmitt, A. V. Setty, F. Sorrentino, C. R. S. Williams, E. Ott, and R. Roy, *Phil. Trans. R. Soc. A* **368**, 343 (2010).
 [23] K. E. Callan, L. Illing, Z. Gao, D. J. Gauthier, and E. Schöll, *Phys. Rev. Lett.* **104**, 113901 (2010).
 [24] D. P. Rosin, K. E. Callan, D. J. Gauthier, and E. Schöll, *Europhys. Lett.* **96**, 34001 (2011).
 [25] B. Ravoori, A. B. Cohen, J. Sun, A. E. Motter, T. E. Murphy, and R. Roy, *Phys. Rev. Lett.* **107**, 034102 (2011).
 [26] See Supplemental Material at <http://link.aps.org/supplemental/10.1103/PhysRevLett.110.064104> for mathematical conditions of stability of group synchrony, comparison of experiment with simulation, and simulations of a seven-node network.
 [27] J. Mulet, C. Mirasso, T. Heil, and I. Fischer, *J. Opt. B* **6**, 97 (2004).
 [28] I. Fischer, R. Vicente, J. M. Buldú, M. Peil, C. R. Mirasso, M. C. Torrent, and J. García-Ojalvo, *Phys. Rev. Lett.* **97**, 123902 (2006).